CEA

(NT)

DEM/
EN VUE D'UNE PUBLICATION OU D

FR9701721

Direction: DSM
Centre: Saclay
Service: DRECAM/SPEC
Réf: S96/051

Titre original du document: Equilibrium properties of proximity effect
(Propriétés à l'équilibre de l'effet de proximité)

AUTEURS	AFFILIATION	Dept/Serv/Sect	VISA
D. Estève	CEA	DRECAM/SPEC	
H. Pothier	CEA	DRECAM/SPEC	
S. Guéron		DRECAM/SPEC	
N.O. Birge		DRECAM/SPEC	
M. Devoret	CEA	DRECAM/SPEC	

Nature du document

Périodique	Conf./Congrès	Ouvrage	Rapport	Thèse	Cours	Mémoire de stage	Autre
☐	☒	☐	☐	☐	☐	☐	☐

Congrès: Les XXXI^{emes} rencontres de Moriond "Correlated Fermions and Transport in Mesoscopic Systems"
Lieu: Les Arcs, France
Date: January 20-27, 1996

FR9701721 → NT 651 IN.FR

Langue: Anglais

Les visas portés ci-dessous attestent que la qualité scientifique et technique de la publication proposée a été vérifiée et que la présente publication ne divulgue pas d'information brevetable, commercialement utilisable ou classée.

	Sigle	Nom	Date	Visa	Observation
Chef de Service	SPEC	J. Hammann	07/10/96		
Chef de Département	DRECAM	F. Gounand	14.10.96		

VOL 28 № 12

FR 9701721

Physique de l'Etat Condensé
SPEC – DRECAM – DSM
CEA – Saclay

S96/051

Equilibrium properties of proximity effect

D. Estève, H. Pothier, S. Guéron, N.O. Birge, M. Devoret
CEA–Saclay, DSM/DRECAM/Service de Physique de l'Etat Condensé
F-91191 Gif-sur-Yvette Cedex, FRANCE

ABSTRACT

The proximity effect in diffusive normal-superconducting (NS) nanostructures is described by the Usadel equations for the electron pair correlations. We show that theses equations obey a variational principle with a potential which generalizes the Ginzburg-Landau energy functional. We discuss simple examples of NS circuits using this formalism. In order to test the theoretical predictions of the Usadel equations, we have measured the density of states as a function of energy in a long N wire in contact with a S wire at one end, at different distances from the NS interface.

Les ~~XXXIèmes~~ 31. rencontres de Moriond "Correlated Fermions and Transport in Mesoscopic Systems"
Les Arcs, France
January 20-27, 1996

EQUILIBRIUM PROPERTIES OF PROXIMITY EFFECT

D. Estève, H. Pothier, S. Guéron, Norman O. Birge* and M. Devoret
Service de Physique de l'Etat Condensé
CEA-Saclay
91191 Gif-sur-Yvette, France

The proximity effect in diffusive normal-superconducting (NS) nanostructures is described by the Usadel equations for the electron pair correlations. We show that these equations obey a variational principle with a potential which generalizes the Ginzburg-Landau energy functional. We discuss simple examples of NS circuits using this formalism. In order to test the theoretical predictions of the Usadel equations, we have measured the density of states as a function of energy in a long N wire in contact with a S wire at one end, at different distances from the NS interface.

I. INTRODUCTION

In a normal-superconducting (NS) nanostructure, the electron pair correlations close to the NS interfaces vary in space and interpolate between those of the S and N reservoirs to which the structure is connected. The present understanding of this proximity effect [1] is based on the theory of non-equilibrium superconductivity [2]. In this theory, the space and energy-dependent correlations between electrons of opposite spin are described by Green functions called $\hat{R}$, $\hat{A}$, $\hat{K}$. The retarded $\hat{R}$ and advanced $\hat{A}$ Green functions describe the quasiparticle energy spectrum and the superconducting condensate, whereas the Keldysh function $\hat{K}$ contains in addition the quasiparticle filling factors. These Green functions obey differential equations called the Usadel equations. At first sight, these equations bear little ressemblance to the Ginzburg-Landau (GL) equation for the superconducting order parameter $\Psi(x)$. This GL equation, which is derived from a variational principle for the GL energy functional, is valid only near the transition temperature and contains no energy dependence [3].

A first aim of this work is to show that the equilibrium Usadel equations for $\hat{R}$ and $\hat{A}$ also derive from a variational principle for a potential which generalizes the GL functional. This variational method extends the framework developed by Nazarov [4] to finite energy and finite magnetic field. It also provides physical insight into the proximity effect, as illustrated by simple examples.

A second aim of this work is to test the predictions of the Usadel equations in a simple geometry. For that purpose, we have measured the quasiparticle density of states $n(x, E)$ as a function of energy in a long N wire in contact with a superconductor at one end, at different distances from the contact, and well below the superconducting transition temperature.

II. GREEN FUNCTIONS DESCRIPTION OF THE PROXIMITY EFFECT AT EQUILIBRIUM

In this section, we summarize the main theoretical results on the proximity effect at equilibrium [6].

A. Parametrization of Green functions on the complex unit sphere

We use the following angular parametrization for the retarded $\hat{R}$ and advanced $\hat{A}$ Green functions:

$$\begin{aligned}\hat{R} &= \cos\theta\tau_z + \sin\theta(\cos\varphi\tau_x + \sin\varphi\tau_y) \\ \hat{A} &= -\cos\bar{\theta}\tau_z + \sin\bar{\theta}(\cos\varphi\tau_x + \sin\varphi\tau_y)\end{aligned} \tag{1}$$

where $\theta(x, E)$ is the complex proximity angle, $\varphi(x)$ the real superconducting phase and τ_x, τ_y, τ_z the usual Pauli matrices. We define the complex unit sphere as the set of points with polar coordinates θ and φ, for complex θ and real φ. The proximity effect in a NS structure can thus be described by assigning to each position x of the circuit and to each energy E a representative point P on the complex unit sphere. At a given energy, these representative points P form a trajectory which is continuous except at tunnel junction interfaces. At a N reservoir, P is located at the north pole of the sphere $\theta = 0$. At a S reservoir, P is located at an angle $\theta = \theta_{BCS}(E)$ with the phase φ of the reservoir. The proximity angle corresponding to the BCS theory is defined by $\sin\theta_{BCS}(E) = \Delta/\sqrt{\Delta^2 - E^2}$ where Δ is the BCS gap. At $E = 0$, $\theta_{BCS} = \pi/2$ and all trajectories lie on the real unit sphere (see Fig. 1).

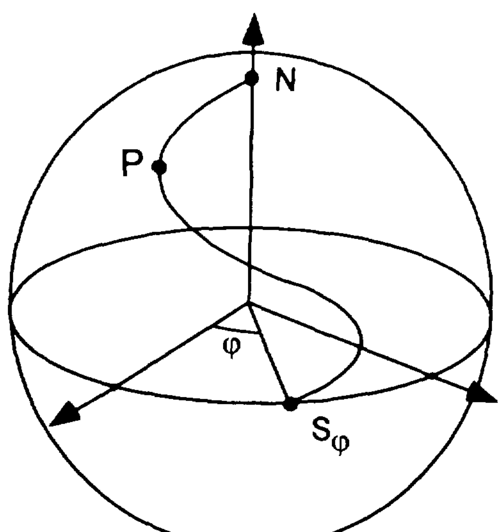

FIG. 1. Representation of the proximity effect: The point P follows a trajectory going from a normal reservoir (N) to a superconducting reservoir with phase φ (S_φ).

B. Density of states

The equilibrium properties of the proximity effect are completely determined by the set of points P. The density of states $n(x, E)$ at position x and at energy E is related to the proximity angle $\theta(x, E)$ by the relation:

$$n(x, E) = n_0 \,\mathrm{Re}\left[\cos\theta(x, E)\right] \qquad (2)$$

where n_0 is the normal density of states at the Fermi level. At thermal equilibrium, the quasiparticle state filling factors are given by the Fermi function $f(E) = \left(1 + \exp\frac{E}{k_B T}\right)^{-1}$ where T is the temperature.

C. Supercurrent density

If the NS structure contains S reservoirs biased at different phases or loops threaded by a magnetic field, equilibrium supercurrents will flow in the sample. Like in a BCS superconductor, the supercurrent density j_S is proportional to the covariant phase gradient:

$$j_S = \left[\frac{\sigma}{4e}\int_{-\infty}^{+\infty} dE \tanh\left(\frac{E}{2k_B T}\right) \mathrm{Im}\left(\sin^2\theta\right)\right]\left(\nabla\varphi + \frac{2e}{\hbar}A\right) \qquad (3)$$

where σ, e, and A are respectively the N state conductivity, the electron charge and the vector potential. $\mathrm{Im}\left(\sin^2\theta\right)$ can be interpreted as the effective density of pairs at energy E.

D. The Usadel equations

We consider here wires with a constant cross section small enough to ensure that the proximity effect depends only on one coordinate x along each wire. For the parametrization (1), the Usadel equations are:

$$\frac{\hbar D}{2}\frac{\partial^2\theta}{\partial x^2} + \left[iE - \frac{\hbar}{2\tau_{in}} - \left(\frac{\hbar}{\tau_{sf}} + \frac{\hbar D}{2}\left(\frac{\partial\varphi}{\partial x} + \frac{2e}{\hbar}A_x\right)^2\right)\cos\theta\right]\sin\theta + \Delta(x)\cos\theta = 0 \qquad (4)$$

$$\frac{\partial}{\partial x}\left[\left(\frac{\partial\varphi}{\partial x} + \frac{2e}{\hbar}A_x\right)\sin^2\theta(\varepsilon)\right] = 0 \qquad (5)$$

where τ_{in} is the inelastic scattering time, τ_{sf} the spin-flip scattering time, A_x the vector potential component along the wire and $\Delta(x)$ the pair potential. The self-consistency equation for $\Delta(x)$ is:

$$\Delta(x) = n_0 V_{eff}\int_0^{\hbar\omega_D} dE \tanh\left(\frac{E}{2k_B T}\right) \mathrm{Im}\sin\theta(x, E) \qquad (6)$$

where V_{eff} is the pairing interaction and ω_D is the Debye frequency.

E. Proximity effect in a N wire in contact with a S wire at one end

We first discuss the simple case of two semi-infinite normal and superconducting wires in contact at $x = 0$. The reservoirs are then located at $x = \pm\infty$. We assume that the contact has a resistance R_T in the normal state. The Usadel equation (4) is thus supplemented with the following boundary conditions: far from the interface, $\theta_N = 0$ in the normal metal, and $\theta_S = \theta_{BCS}$ in the superconductor. At the interface,

$$\sigma_{N,S}\left(\frac{\partial\theta_{N,S}}{\partial x}\right)_{x=0} = (aR_T)^{-1}\sin\left(\theta_S(0,E) - \theta_N(0,E)\right) \tag{7}$$

where σ_X is the normal state conductivity of electrode X, R_T is the interface resistance and a is the contact area [7]. In the case of a good contact, $\theta_S(0,E) = \theta_N(0,E)$. The resolution of the Usadel equation is greatly simplified if Δ is assumed to be independent of x in the superconductor, since Eq. (4) then has a first integral:

$$\frac{\hbar D}{4}\left(\frac{\partial\theta}{\partial x}\right)^2 - \left(iE - \frac{\hbar}{2\tau_{in}}\right)\cos\theta + \frac{\hbar}{4\tau_{sf}}\cos 2\theta + \Delta\sin\theta = F(E) \tag{8}$$

The proximity angle θ is obtained by a second integration performed numerically. A numerical self-consistent resolution of Equations (4, 6) has recently been performed [8]. Analytical expressions can be obtained in various limits [6]. In particular, the proximity angle has a universal form at distances x from the contact such that $L_\Delta = \sqrt{\hbar D/\Delta} \ll x \ll \sqrt{D\tau_{sf}}, \sqrt{D\tau_{in}}$:

$$\theta = 4\arctan\left[\left(\sqrt{2}-1\right)\exp\left((i-1)\sqrt{\frac{E}{E_C}}\right)\right] \tag{9}$$

where $E_C = \hbar D/x^2$. In this regime, the reduced density of states $n(x,E)/n_0$ is a universal function $\rho(\epsilon)$ of the reduced energy $\epsilon = E/E_C$ (see Fig. 2).

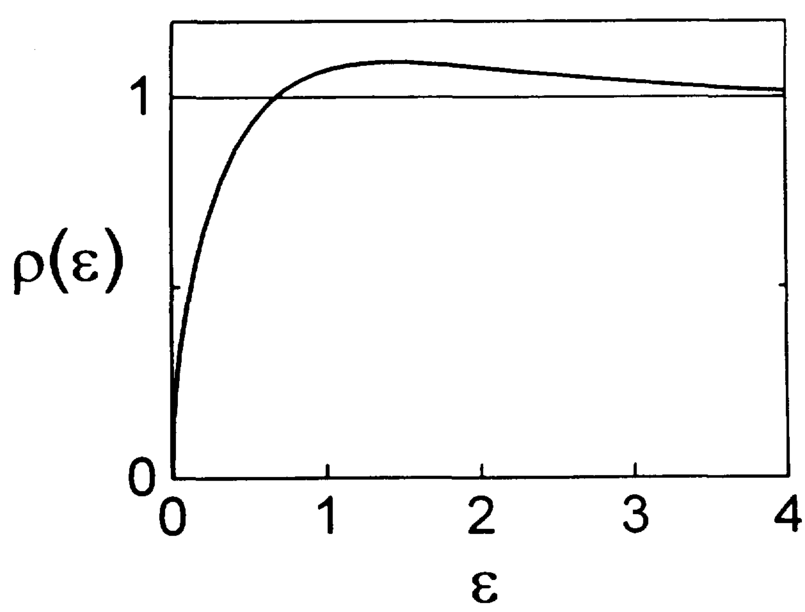

FIG. 2. Reduced density of states $\rho(\varepsilon)$ in the universal regime. The density of states in the wire at distance x and at energy E is $n(x,E) = n_0\rho(E/E_C)$.

III. A VARIATIONAL PRINCIPLE FOR THE USADEL EQUATIONS

A. The effective potential U

We define the following dimensionless potential:

$$U = \int_{vol.} dv\; n_0 \left[\frac{\hbar D}{4} \left(\frac{ds}{dx} \right)^2 - \left(iE - \frac{\hbar}{2\tau_{in}} \right) \cos\theta - \frac{\hbar}{\tau_{sf}} \frac{\sin^2\theta}{2} + \Delta(x) \sin\theta \right] \tag{10}$$

where the distance s is defined by the gauge invariant metric:

$$ds^2 = d\theta^2 + (d\varphi - d\varphi_A)^2 \sin^2\theta \tag{11}$$

with $d\varphi_A = -\frac{2e}{\hbar} A_x.dx$. The integral is taken over the volume of the sample. The phase field $\varphi_A(x)$ results from the applied magnetic field but also from the field produced by the S currents in the structure. We will assume in the following that the S currents are too small to significantly screen the applied magnetic field and that $\varphi_A(x)$ is an externally applied phase field in a given gauge. The first term of U can be understood as a tension on the trajectory of the representative points P, while the other terms are potential terms.

B. The variational principle

It is straightforward to check that the variational equation $\delta U = 0$ with respect to θ and φ yields the Usadel equations (4-5). The set of Usadel equations at all energies generalize the G-L equation for Ψ. Like in the GL energy functional whose minimisation leads to the GL equation, u is the sum of the square of a covariant gradient term and of potential terms. At a given energy, the global potential U is a functional of the trajectories followed by the representative points P on the complex unit sphere. This treatment provides a physical insight into the different terms appearing in the Usadel equations and is a direct way to solve numerically the Usadel equations.

C. The proximity effect at zero energy

The Usadel equations can be solved in two steps. The phase φ can be determined first by solving the equations (4-5) at zero energy, where they have a simpler form. The proximity angle θ is then determined by solving (4). The Usadel equations at zero energy thus play a special role. The solution is further simplified if the length of the mesoscopic structure is smaller than the phase coherence length $L_\varphi = \min\left[\sqrt{D\tau_{sf}}, \sqrt{D\tau_{in}}\right]$ and if the connection pads are good N or S reservoirs. In that case, the trajectories which minimize the global potential are the geodesics of the unit sphere with the metric (11). The global potential U_0 at zero energy of a N wire of resistance R with representative end points P and Q is thus simply :

$$U_0 = \left(\frac{R_K}{4\pi R} \right) \frac{\mathcal{L}^2}{2} \tag{12}$$

where $R_K = h/e^2$ and where $\mathcal{L}$ is the gauge invariant length of the arc PQ. In the absence of a magnetic field, $\mathcal{L}$ is simply the length of the arc PQ. A magnetic field acts as an extra rotation field which affects the length of a trajectory in the same way that winds modify the effective distances planes must travel around the earth. The length $\mathcal{L}$ is in this case the length of the arc

PQ′ where Q′ is at the same latitude as Q but at a longitude increased by $(\varphi_A(Q) - \varphi_A(P))$. In the case of a tunnel junction of normal state tunnel resistance R_T instead of a wire, the contribution to the global potential takes the form:

$$U_0' = \left(\frac{R_K}{4\pi R_T}\right)\frac{\gamma^2}{2} \tag{13}$$

where $\gamma^2 = 2(1 - \cos\mathcal{L})$ is the square of the geometrical distance between the representative points of both sides of the junction.

The global potential for the whole structure is simply the sum of the contributions of the different elements. Finding the minimum of the global potential is equivalent to finding the equilibrium positions of a set of springs with the following correspondence rules:

-Each wire R (resp. each tunnel junction R_T) is represented by a spring of stiffness constant R^{-1}(resp. R_T^{-1}).

-The springs are connected in the same way as the elements they correspond to. The arcs of springs forming a loop are modified as explained above.

-A wire-type spring is constrained to lie on the unit sphere.

-A junction-type spring lies along the cord joining its end points.

These rules are equivalent to the conservation law of the spectral current at the nodes found by Nazarov [4]. The determination of the angles θ and φ at zero energy gives the density of states at zero energy (2) and allows one to calculate the transport properties at zero temperature. Nazarov has shown that the resistance of a NS circuit at zero temperature is obtained by applying the usual rules to the same circuit but with a shunt installed between all the superconducting electrodes, renormalized junction resistances $R_T^{ren} = R_T \cos\mathcal{L}$ and unchanged diffusive wire resistances. The resistance one calculates using these rules can be surprising, as examplified by the circuit shown in Fig. 3: the resistance between the N and S reservoirs depends on the diffusive resistance connected to the dangling S' reservoir.

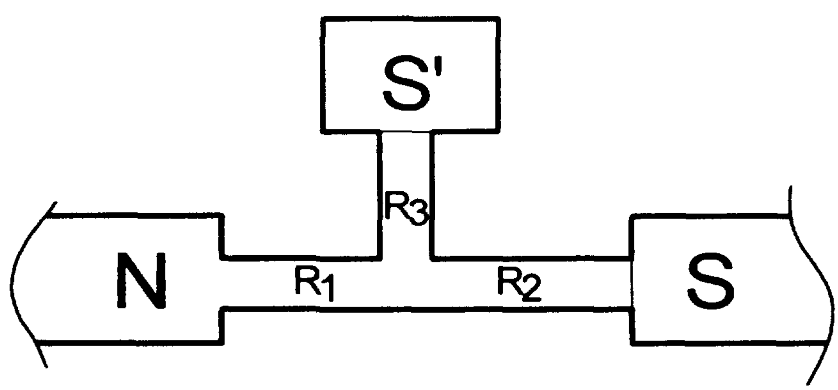

FIG. 3. Example of diffusive NS structure in which the resistance is strongly modified by the proximity effect. The resistance R between the N and S reservoirs $R = R_1 + \left(R_2^{-1} + R_3^{-1}\right)^{-1}$ depends on the resistance R_3 of the dangling arm.

A simple circuit with a loop and its representation on the unit sphere are shown in Fig. 4a. When the loop encloses a flux Φ, the two springs associated with the two branches of the loop follow different arcs. The effective length of the two arcs is $\mathcal{L}_{A'B} = \mathcal{L}_{A''B}$. The opening angle between A' and A'' is $\varphi = 2\pi\Phi/\Phi_0$, where $\Phi_0 = h/2e$ is the flux quantum. The total potential U of the circuit is the sum of the potentials (12) of the four branches. The proximity angles at nodes A and B can easily be determined by minimizing the potential U. The variations of θ_A and θ_B with the flux Φ are shown in Fig. 4b in the particular case of equal resistances R_{NA}, R_{AB} and R_{BS}.

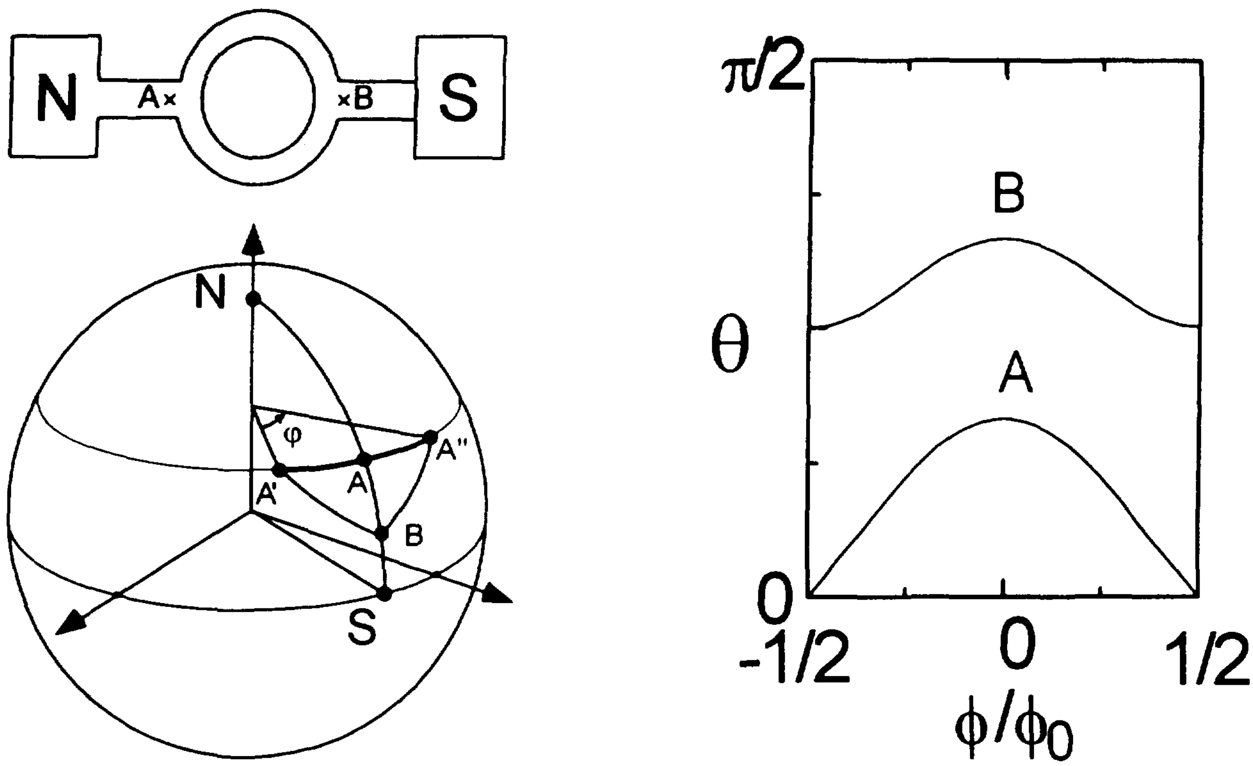

FIG. 4. a) Simple NS circuit with a loop enclosing a flux Φ and its representation on the unit sphere. b) Variations of the proximity angle θ at points A and B as a function of the flux Φ.

D. The proximity effect at finite energy

We have used the variational formalism to find the solution of the Usadel equations in the case of a short wire between two N and S reservoirs (see Fig. 5). The direct integration of the Usadel equations is not straightforward because the boundary conditions are given at two different positions. The variational calculation is an efficient way to circumvent this difficulty. The variations of the complex proximity angle θ with the position x along a wire of length $L = 5L_\Delta$ are shown in Fig. 5 for different values of the energy.These results are necessary to calculate the slight decrease of the resistance at intermediate temperatures, as discussed in ref. [5]. In the case of a $L = 5L_\Delta$ long wire, we calculate that the resistance is reduced by 3% at its minimum which occurs at a temperature $T \simeq 0.25\ \Delta/k_B$.

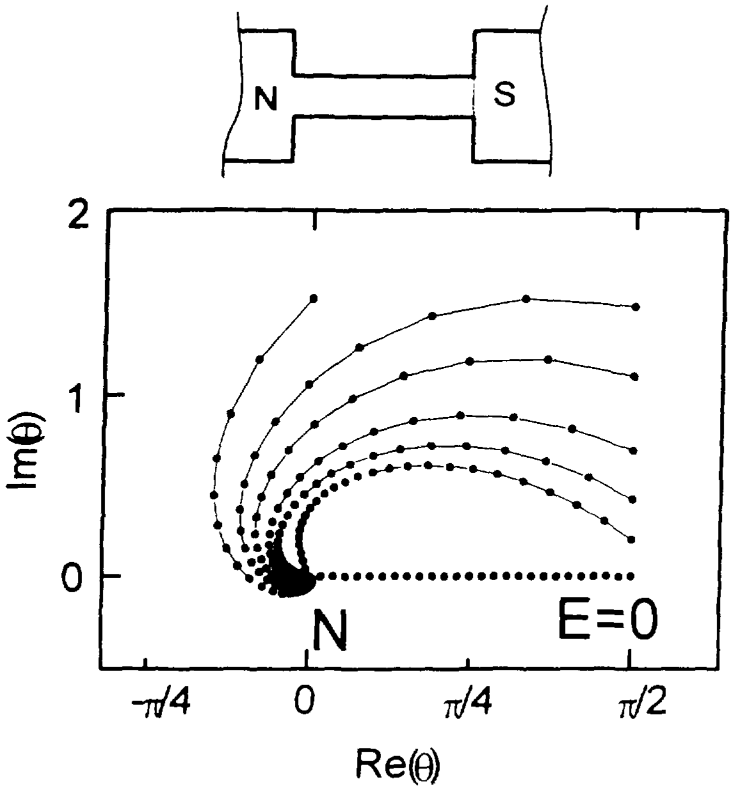

FIG. 5. Variations of the proximity angle θ along a N wire of length $L = 5L_\Delta$ connected at its ends to a normal and to a superconducting reservoir. The distance between successive points is $0.2L_\Delta$. The energies are $E/\Delta = 0, 0.2, 0.4, 0.6, 0.8, 0.9, 1.1$.

IV. EXPERIMENTAL TEST OF THE USADEL PREDICTION FOR THE DENSITY OF STATES

In this section, we test the predictions of the Usadel equation (4) for the density of states $n(x, E)$ given by (2) in the simple geometry discussed in section II-E.

A. Experimental setup

We have measured the tunneling density of states in a N wire in good contact with a S wire at one end. Tunneling has been used extensively to measure the density of states [9]: at zero temperature, the differential conductance $dI/dV(V)$ of a tunnel junction between a normal metal electrode and a metal with a density of states $n(E)$ is, disregarding single-electron charging effects [10], proportional to $n(eV)$. Figure 6 shows a photograph of our sample, which consists of two similar circuits. On the bottom one, two copper electrodes (called "fingers" in the following, and labeled F_1 and F_3), are in contact through very opaque tunnel barriers (resistances in the MΩ range) with a normal wire N, whose left end makes an overlapping contact with a superconductor S. On the top circuit, a single finger, labeled F_2, is placed at an intermediate distance from the NS contact, between F_1 and F_3. The three fingers, positioned 200, 300 and 800 nm from the left end of the normal wire, constitute the tunneling spectroscopy probes. Since the quality of the NS contact is known to be a critical parameter in the proximity effect [1], all the layers were deposited through a suspended mask in a single vacuum process [11]. The mask, made of germanium, was fabricated by e-beam lithography with reactive ion etching. We first evaporated 20 nm of aluminum perpendicularly to the mask in order to obtain the S superconducting electrode. We then immediately evaporated 25 nm of copper at an angle to obtain the N normal wire. The angle was chosen so as to produce an overlap with the aluminum electrode on the left, presumably making a good contact. The insulating barrier was grown from two 1.4 nm-thick layers of aluminum oxidized in a 80 mbar O_2 (10%) Ar (90%) mixture for 10 minutes. Lastly, we evaporated 30 nm of copper at an angle to produce the fingers $F_{1,2,3}$. In order to separate the three shadows of the mask, the MAA resist layer carrying the germanium mask was overetched. This was obtained with a low-dose pre-exposure of the sample around the normal wires and the fingers. The parasitic replicas on both sides of the superconducting electrode produced by the angle evaporations were lifted off in the non-overetched regions. A reference NS tunnel junction and a long and narrow NS sandwich were simultaneously fabricated on the chip. The former was used to measure the unperturbed density of states in the superconducting film while the critical temperature of the latter provided a lower limit for the transparency of the NS contact. The sample was mounted in a copper box thermally anchored to the mixing chamber of a dilution refrigerator. Measurements were performed through properly filtered coaxial lines [12].

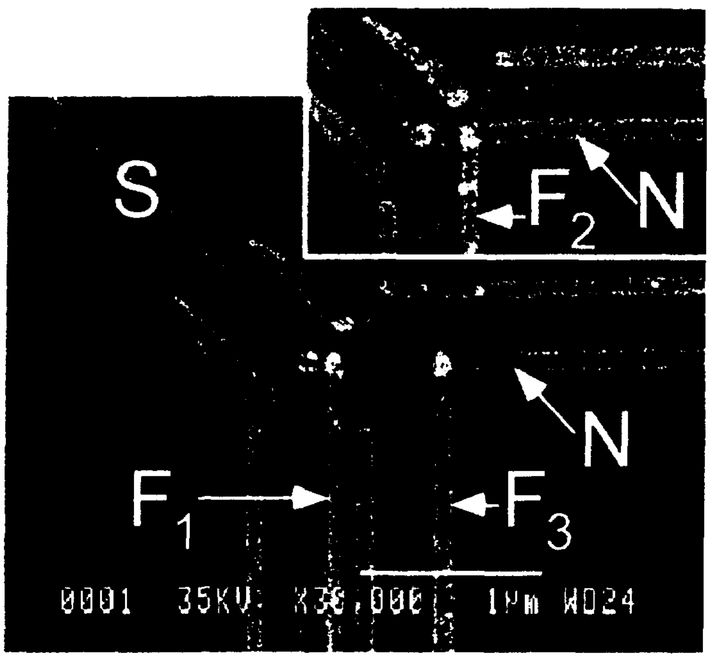

FIG. 6. SEM photograph of the sample: a normal (copper) wire N, horizontal, is in good contact with a superconducting (aluminum) wire S, diagonal on the left, at their overlap. Two normal (copper) fingers, vertical, labelled F_1 and F_3, are connected to the wire through very opaque tunnel barriers. The density of states in the normal wire is given by the differential conductance of the tunnel junction as a function of voltage. On a similar device, a third finger, labelled F_2, is placed at an intermediate distance.

B. Measurements of the tunneling density of states

Using lock-in detection, we measured the differential conductance dI/dV of each of the three probe junctions as a function of the voltage V applied between the finger and the right end of the normal wire. The differential conductance displayed a V-shaped groove at low voltages, which became less pronounced at larger distances from the interface. This behavior is shown in Fig. 7 where we plot the $dI/dV\,(V)$ characteristic of the F_1, F_2 and F_3 junctions, taken at 20 mK.

We have multiplied each trace by the resistance $R_i = (dI/dV)^{-1}$ measured at $V = 0.3$ meV.

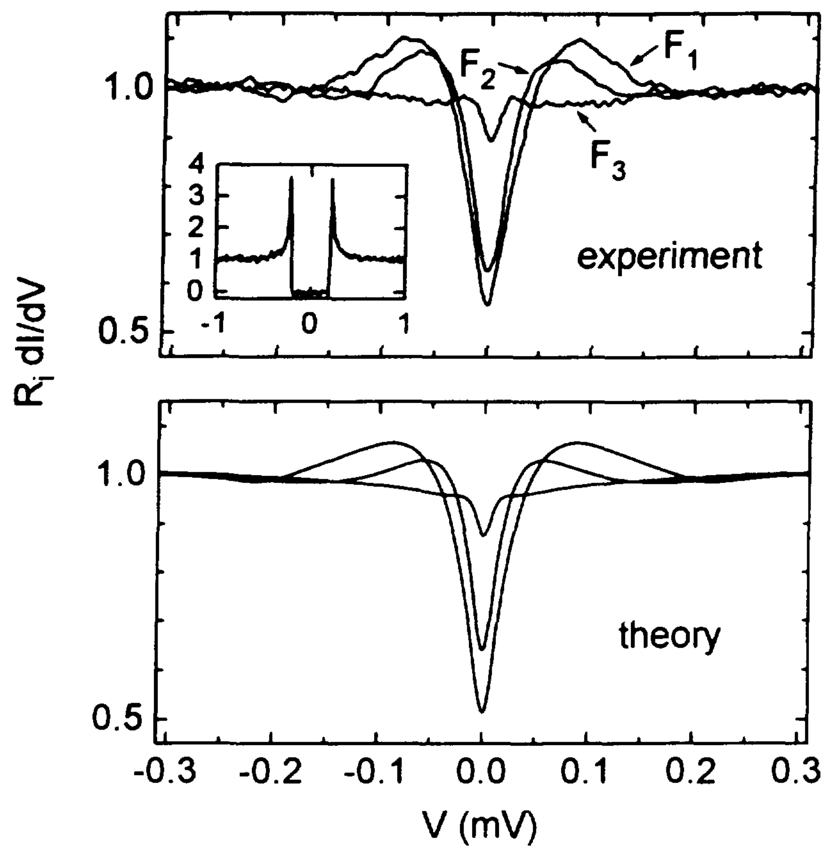

FIG. 7. Top panel: differential conductance of the tunnel junctions at F_1, F_2 and F_3 as a function of the applied voltage V, taken at 20 mK. The data were normalized by the differential conductance at $V = 0.3$ mV. Inset, differential conductance of the reference NS tunnel junction. Bottom panel: predicted differential conductance at the three distances to the NS contact obtained from the convolution of the density of states calculated from the Usadel equation (Eq. (4)) with the function $P(E)$ which describes the Coulomb blockade at the junctions. We used $\Delta = 0.212$ meV for the gap of aluminum, $D = 70 \times 10^{-4}$ m^2/s for the diffusion constant of copper, and $\gamma_{sf} = 1.5 \times 10^{10}$ s^{-1} for the spin-flip scattering rate.

The differential conductance of the reference NS tunnel junction (inset of Fig. 7) is well fitted by a BCS density of states for the superconducting electrode and yields the energy gap $\Delta = 0.212$ meV.

We repeated the differential conductance measurement of the three fingers with an external magnetic field perpendicular to the chip. In Fig. 8 we present the F_1 data taken at $T =$ 30 mK for $H = 0$, 0.06, and 0.1 T. As the field is increased, the groove structure progressively disappears and, above 0.1 T, only a weak, broad-winged, field-independent structure remains. This structure, which extends to 3 mV, is the same for the three fingers. We attribute it, as explained below, to single-electron charging effects. When the temperature was increased (data not shown), the groove structure was progressively washed out, whereas the high-field shape was unaffected.

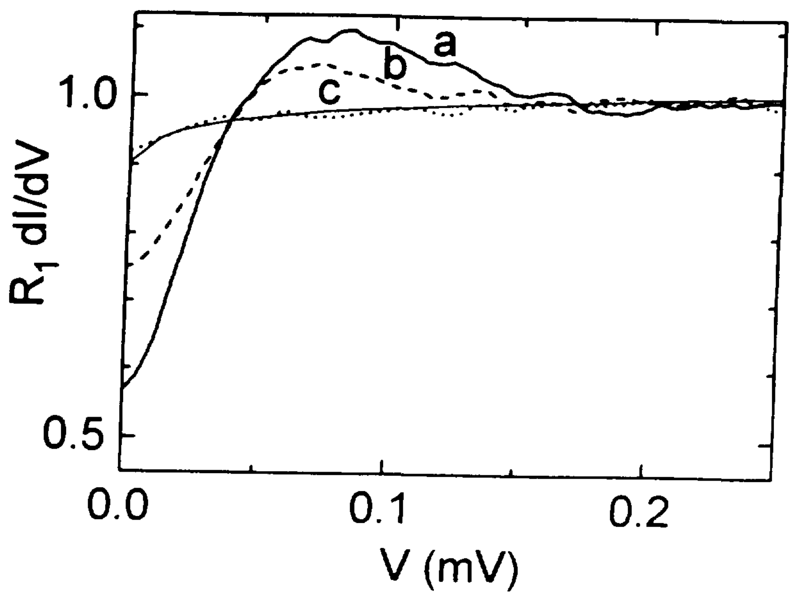

FIG. 8. Differential conductance as a function of the voltage V measured at 30 mK and in a magnetic field $H = 0$ (curve a), 0.06 T (curve b), and 0.1 T (curve c). The thin solid line is a fit of curve c using Eq. (14), in which the DOS $n(x, E)$ was taken constant. It accounts for the influence of single-electron charging effects on the conductance of a tunnel junction between normal electrodes.

C. Calculation of the tunneling density of states

We have calculated the tunneling density of states assuming that the NS contact is a good contact. Although the tunnel conductance G_T of the NS contact is not measured, the absence of superconductivity in the sandwich down to 18 mK provides a lower limit: $G_T > 2$ S. With such a high conductance, the perfect contact approximation $\theta_S(0, E) = \theta_N(0, E)$ is valid. We used in the numerical calculations the value of Δ given by the measurement of the reference NS tunnel junction and the diffusion constant $D_N = 70 \times 10^{-4}$ m^2/s in copper deduced from the conductivity of the wire between F_1 and F_3. The spin-flip scattering rate τ_{sf}^{-1} was taken as an adjustable parameter and the inelastic rate was assumed to be negligible. To account for the finite extension of the overlapping NS contact, we assumed that the effective NS interface ($x = 0$) is positioned 20 nm away from the extremity of the normal wire, in the overlap region, and calculated the density of states at the position of the center of each finger.

For quantitative comparison of the Usadel theory with the experimental data, we must take into account the influence of single-electron charging effects on the conductance. At zero temperature, the differential conductance of the probe tunnel junction at a finger is related to the density of states through

$$\frac{dI}{dV} = \frac{1}{R_t} \int_0^{eV} n(x, E)\, P(eV - E)\, dE \tag{14}$$

where R_t is the tunnel resistance of the junction and $P(E)$ is the probability for the electromagnetic environment of the tunnel junction to absorb an energy E [10]. Finite but low temperatures can be accounted for by convolving expression (14) with the derivative of the Fermi function. For a tunnel junction of capacitance C in series with a resistance R such that

$\alpha = 2R/(h/e^2) \ll 1$, $P(E) = \alpha/E_0\,(E/E_0)^{\alpha-1}$ for E smaller than $E_0 = e^2/\pi\alpha C$. The high field data for F_1, F_2 and F_3 are well fitted by Eq. (14) with $n(x,E)$ constant (see fit of curve (c) in Fig. 8), and yield $\alpha = 0.022$. The fit corresponds to $R = 300\ \Omega$ and $C = 1$ fF, in good agreement with the estimated values.

D. Comparison between experiment and theory

The comparison between the zero field data taken at 20 mK for the three fingers F_1, F_2 and F_3, and the prediction of Eq. (14) calculated with the density of states $n(x, E)$ previously discussed is shown in the bottom panel of Fig. 7. The calculation is performed with the value $\tau_{sf}^{-1} = 1.5 \times 10^{10}\ s^{-1}$ which provides the best overall agreement. As seen in the figure, the theoretical curves reproduce the general features of the experimental data, especially the evolution of the characteristic energy scale with distance from the NS interface. The present theory does not produce maxima as pronounced as those observed, but the exact resolution of the Usadel equation (4) including the gap self-consistency equation (6) improves the agreement [8].

V. CONCLUSION

We have shown that the equilibrium Usadel equations obey a variational principle. This approach, which generalizes the G-L formalism, is an extension of the theory previously developed by Nazarov. At zero energy, the variational principle corresponds to minimizing the effective length of a trajectory on the unit sphere. At finite energy, the variational principle can be used to solve numerically the Usadel equations. We have tested the predictions of the Usadel equations for the density of states in a normal wire in contact at one end with a superconducting wire. The measured tunneling density of states at three distances from the contact is in good agreement with the theoretical predictions.

---

* On leave from Michigan State University, East Lansing, MI 48824, USA.

[1] G. Deutscher and P. G. de Gennes, in *Superconductivity*, edited by R. D. Parks (Marcel Dekker, New York, 1969), p. 1005.

[2] A. Schmid, in *Nonequilibrium Superconductivity, Phonons, and Kapitza Boundaries*, edited by K. E. Gray (Plenum Press, New York, 1981), p. 423; J. Rammer and H. Smith, Rev. Mod. Phys. **58**, 323 (1986); A. I. Larkin and Yu. N. Ovchinikov, in *Nonequilibrium Superconductivity*, edited by D. N. Langenberg and A. I. Larkin (North Holland, Amsterdam, 1986), p. 493; K. D. Usadel, Phys. Rev. Lett. **25**, 507 (1970).

[3] M. Tinkham, *Introduction to Superconductivity* (Mc Graw Hill, 1985), chapter 4.

[4] Yu. V. Nazarov, Phys. Rev. Lett. **73**, 1420 (1994); T. H. Stoof and Yu. Nazarov, preprint.

[5] Yu. V. Nazarov and T. H. Stoof, Phys. Rev. Lett. **76**, 823 (1996).

[6] A. F. Volkov, A. V. Zaitsev, and T. M. Klapwijk, Physica (Amsterdam) **210C**, 21 (1993); A. F. Volkov, Phys. Rev. Lett. **74**, 4730 (1995); F. Zhou, B. Spivak, and A. Zyuzin, Phys. Rev. B **52**, 4467 (1995).

[7] S. Yip, Phys. Rev. B **52**, 15504 (1995).

[8] W. Belzig and C. Bruder, preprint.

[9] J. M. Rowell, in *Tunneling Phenomena in Solids*, edited by E. Burstein and S. Lundqvist (Plenum, New York, 1969), p. 385; T. Claeson, ibid., p. 443.
[10] M. H. Devoret, D. Esteve, H. Grabert, G.-L. Ingold, H. Pothier, and C. Urbina, Phys. Rev. Lett. **64**, 1824 (1990); G.-L. Ingold and Yu. V. Nazarov, in *Single Charge Tunneling*, edited by H. Grabert and M.H. Devoret (Plenum Press, New York, 1992), p. 21.
[11] G. J. Dolan and J. H. Dunsmuir, Physica B **152**, 7 (1988).
[12] D. Vion, P.F. Orfila, P. Joyez, D. Esteve, and M. H. Devoret, J. Appl. Phys. **77**, 2519 (1995).

PROPRIÉTÉS À L'ÉQUILIBRE DE L'EFFET DE PROXIMITÉ

L'effet de proximité dans les structures diffusives normal-supraconducteur (NS) est décrit par les équations d'Usadel pour les corrélations de paires d'électrons. Nous montrons que ces équations obéissent à un principe variationnel avec un potentiel qui généralise la fonctionnelle d'énergie de Ginzburg-Landau. Nous discutons quelques exemples de circuits NS simples à l'aide de ce formalisme. Pour tester les prédictions des équations d'Usadel, nous avons mesuré la densité d'états en fonction de l'énergie dans un long fil N en contact avec un fil S à un bout, à différentes distances de l'interface NS.